American Physiological Society | AMERICAN JOURNAL OF PHYSIOLOGY Heart and Circulatory Physiology

PUBLISHED ARTICLE
ARCHIVES
SUBSCRIPTIONS
SUBMISSIONS
CONTACT US

Am J Physiol Heart Circ Physiol. 2019 Feb 1; 316(2): H371–H379.
Published online 2018 Nov 30.
doi: 10.1152/ajpheart.00486.2018: 10.1152/ajpheart.00486.2018
Cardiac Excitation and Contraction

PMCID: PMC6397388
PMID: 30499712

Atrial fibrillation and electrophysiology in transgenic mice with cardiac-restricted overexpression of FKBP12

Zhenwei Pan,[1,2] Tomohiko Ai,[2] Po-Cheng Chang,[2,4] Ying Liu,[3] Jijia Liu,[3,5] Mitsunori Maruyama,[2] Mohamed Homsi,[2] Michael C. Fishbein,[6] Michael Rubart,[3] Shien-Fong Lin,[2] Deyong Xiao,[7] Hanying Chen,[3] Peng-Sheng Chen,[2] Weinian Shou,[3] and Bai-Yan Li[1,3]

[1]Department of Pharmacology, Harbin Medical University, Heilonjiang, China
[2]Krannert Institute for Cardiology and the Division of Cardiology, Indiana University School of Medicine, Indianapolis, Indiana
[3]Wells Center for Pediatric Research, Indiana University School of Medicine, Indianapolis, Indiana
[4]The Second Section of Cardiology, Departments of Medicine, Chang Gung Memorial Hospital and Chang Gung University School of Medicine, Taoyuan, Taiwan
[5]The Second Xiangya Hospital, South Central University School of Medicine, China
[6]Department of Pathology and Laboratory Medicine, University of California, Los Angeles, California
[7]Fountain Valley Biotechnology, Inc., Dalian Hi-Tech District, Dalian, China
Corresponding author.
Address for reprint requests and other correspondence: W. Shou, Wells Center for Pediatric Research, Dept. of Pediatrics, Indiana Univ. School of Medicine, Indianapolis, IN (e-mail: wshou@iu.edu).

Received 2018 Jul 18; Revised 2018 Nov 19; Accepted 2018 Nov 19.

Abstract

Cardiomyocyte-restricted overexpression of FK506-binding protein 12 transgenic (αMyHC-FKBP12) mice develop spontaneous atrial fibrillation (AF). The aim of the present study is to explore the mechanisms underlying the occurrence of AF in αMyHC-FKBP12 mice. Spontaneous AF was documented by telemetry in vivo and Langendorff-perfused hearts of αMyHC-FKBP12 and littermate control mice in vitro. Atrial conduction velocity was evaluated by optical mapping. The patch-clamp technique was applied to determine the potentially altered electrophysiology in atrial myocytes. Channel protein expression levels were evaluated by Western blot analyses. Spontaneous AF was recorded in four of seven αMyHC-FKBP12 mice but in none of eight nontransgenic (NTG) controls. Atrial conduction velocity was significantly reduced in αMyHC-FKBP12 hearts compared with NTG hearts. Interestingly, the mean action potential duration at 50% but not 90% was significantly prolonged in αMyHC-FKBP12 atrial myocytes compared with their NTG counterparts. Consistent with decreased conduction velocity, average peak Na^+ current (I_{Na}) density was dramatically reduced and the I_{Na} inactivation curve was shifted by approximately +7 mV in αMyHC-FKBP12 atrial myocytes, whereas the activation and recovery curves were unaltered. The $Na_v1.5$ expression level was significantly reduced in αMyHC-FKBP12 atria. Furthermore, we found increases in atrial $Ca_v1.2$ protein levels and peak L-type Ca^{2+} current density and increased levels of

fibrosis in αMyHC-FKBP12 atria. In summary, cardiomyocyte-restricted overexpression of FKBP12 reduces the atrial $Na_v1.5$ expression level and mean peak I_{Na}, which is associated with increased peak L-type Ca^{2+} current and interstitial fibrosis in atria. The combined electrophysiological and structural changes facilitated the development of local conduction block and altered action potential duration and spontaneous AF.

NEW & NOTEWORTHY This study addresses a long-standing riddle regarding the role of FK506-binding protein 12 in cardiac physiology. The work provides further evidence that FK506-binding protein 12 is a critical component for regulating voltage-gated sodium current and in so doing has an important role in arrhythmogenic physiology, such as atrial fibrillation.

Keywords: action potential duration, cardiac electrophysiology, fibrosis, ion channels, patch clamp, voltage-gated sodium current

INTRODUCTION

Atrial fibrillation (AF) is the most common type of cardiac arrhythmia and is associated with substantial morbidity and mortality (11, 13). Ion channelopathies are major contributing factors to AF (2). Among the different ionic currents, abnormal Na^+ currents (I_{Na}) are known to be causally related to AF (5, 9). Na^+ channel remodeling is a typical pathophysiological alteration that occurs in AF (28, 35). Cardiac voltage-gated Na^+ channels determine the amplitude and slope of the action potential (AP) upstroke in atrial and ventricular cardiomyocytes and are responsible for the generation of the inward I_{Na} that underlies excitability and conduction in the working myocardium and conduction system cells (8). Mutations in genes encoding cardiac voltage-gated Na^+ channels (e.g., SCN5A) and their functional regulators are associated with multiple forms of arrhythmogenic syndromes (23) and AF (9). Six percent of AF cases are associated with rare genetic variants of SCN5A, a gene coding the $Na_v1.5$ α-subunit (7). For example, the loss-of-function mutation (e.g., Brugada syndrome) (3) and gain-of-function mutation of cardiac voltage-gated Na^+ channels are both associated with familial AF (23). Transgenic mice with overexpression of loss-of-function mutant *SCN5A* display spontaneous AF (33), highlighting the importance of I_{Na} in the generation of AF.

Recently, we identified a novel physiological function for FK506-binding protein 12 (FKBP12) in regulating cardiac voltage-gated Na^+ channels. FK506 (Tacrolimus) is a potent immunosuppressant drug and is used to prevent host-to-donor tissue rejection in organ transplant patients. However, it has been well documented that FK506 causes arrhythmias, including sinus arrest, long QT syndrome, and sudden death (6, 12, 25), yet the mechanism of this action is not clear. FKBP12 is a cytoplasmic peptidyl-prolyl *cis-trans* isomerase and is highly expressed in cardiomyocytes. Previously, it has been shown that FKBP12 regulates the skeletal muscle Ca^{2+}-release channel ryanodine receptor (RyR)1 and excitation-contraction coupling in skeletal muscle (18). However, its function in cardiomyocytes was largely unknown, although FKBP12 is highly expressed in both atrial and ventricular myocytes. Previously, we have shown that ablation of FKBP12 in the heart leads to a greater than twofold increase in peak I_{Na} density in mouse ventricular cardiomyocytes; in contrast, ventricular cardiomyocytes isolated from transgenic mice with cardiac-restricted overexpression of FKBP12 (αMyHC-FKBP12) exhibited a dramatic reduction in peak I_{Na} density and showed significantly reduced ventricular conduction velocity (17). These data suggest that FKBP12 is an important regulator for $Na_v1.5$.

In addition to changes in the ventricles, we recently found that αMyHC-FKBP12 mice also develop AF during electrophysiological studies and during telemetry ECG monitoring. It has been shown that functional and anatomic reentries are important mechanisms for the occurrence of AF. Either increased atrial size or shortened impulse wavelength by decreased conduction velocity and/or refractory period

facilitates the formation of multiple wavelets and occurrence of AF (2). The present study aimed to explore potential mechanism that underlies the development of spontaneous AF in these mice. Specifically, we performed a series of optical mapping and patch-clamp experiments and found several unique alterations in electrophysiology and histology in αMyHC-FKBP12 atria that may explain the occurrence of AF in αMyHC-FKBP12 hearts.

METHODS

αMyHC-FKBP12 mice. The animal study protocols were approved by the Institutional Animal Care and Use Committee of Indiana University and the Methodist Research Institute and conformed with the National Institutes of Health *Guide for the Care and Use of Laboratory Animals*. The αMyHC-FKBP12 transgenic mice used in this study were generated as previously described (17). The mice used for monitoring and optical mapping were 2–4 mo old.

Telemetric ECG analyses. Telemetric analysis of ECGs was performed on the PhysioTel Telemetry system (Data Sciences, St. Paul, MN) (17). Briefly, mice were lightly anesthetized with 1.5% isoflurane. The subcutaneous leads were surgically placed over the scapula in a lead II configuration. The continuous data recordings were allowed using hardware modification in the waveform format from multiple instrumented mice. The data were collected using an implantable radiofrequency microtransmitter (TA1010ETA-F20) and then analyzed using Dataquest A.R.T. version 4.1.

Optical mapping experiment in Langendorff-perfused hearts. Hearts were perfused with a Langendorff perfusion system with 37°C Tyrode solution [containing (in mmol/l) 125 NaCl, 4.5 KCl, 1.8 NaH_2PO_4, 24 $NaHCO_3$, 1.8 $CaCl_2$, 0.5 $MgCl_2$, and 5.5 glucose] with pH equilibrated to 7.40 ± 0.05 at a flow rate of ≈2 ml/min. Optical mapping of voltage-dependent signals was performed to measure atrial conduction velocities as previously described (17) with minor modifications. The emitted fluorescence was collected using a high-speed CMOS camera (MiCAM Ultima, BrainVision, Tokyo, Japan) at 0.2 ms/frame and 100 × 100 pixels with spatial resolution of 0.07 × 0.07 mm^2/pixel. The preparation was paced from the edge of the right atrial appendage. The conduction time from the stimulus to the completion of the activation of both atria was determined. The conduction velocity was the ratio between the distance from the pacing site to the site of the latest atrial activation and the activation time.

Cell isolation. Left atrial and ventricular cardiomyocytes were isolated from Langendorff-perfused mouse hearts as previously described (16). Single rod-shaped cells with clear cross striations were used for electrophysiological recording. We used only left atrial cardiomyocytes to keep the electrophysiological and biological consistency of cells from each experiment.

Whole cell patch-clamp recording. Whole cell patch-clamp recordings were performed with an Axopatch 700B amplifier (Axon Instruments). I_{Na} was recorded at room temperature (~22°C). Ca^{2+} currents were recorded at 37°C. Tetrodotoxin (5 μM) was added to block I_{Na} when recording Ca^{2+} currents. AP duration (APD) was recorded at 37°C under current-clamp mode in normal Tyrode solution. Current-amplitude data of each cell were normalized to its cell capacitance (current density; in pA/pF), and the current-voltage (*I-V*) relationship (*I-V* curve) was plotted. Voltage-dependent activation and steady-state inactivation profiles were fitted to the following Boltzmann equation: $a = 1/\{1 + \exp[-(V_m - V_{½})/k]\}$, where a is the normalized conductance, V_m is the test potential, $V_{½}$ is the potential at which current is half activated/inactivated, and k is the slope factor.

Western blot. Western blots were performed as previously described (17). Rabbit polyclonal FKBP12 antibody (catalog no. ab2918, 1:2,000) was from Abcam. Rabbit polyclonal $Ca_v1.2$ antibody (catalog no. C1241, 1:200) was from Sigma. Antibody against $Na_v1.5$ (1:1,500) was kindly provided by Dr. Peter Mohler (Ohio State University).

Histological analyses. Hearts were fixed with 10% neutral buffered formalin. Tissues were processed routinely and embedded in paraffin. Sections were stained with hematoxylin and eosin or picrosirius red for histological examination. Custom-written Magic Wand software was used to identify and quantitate the extent of fibrosis.

Statistical analysis. Continuous variables are presented as means ± SE. Nonparametric tests were used to compare the means between groups. Fisher's exact test was used to compare the occurrence of AF between groups. $P \leq 0.05$ was considered statistically significant.

RESULTS

Paroxysmal AF in αMyHC-FKBP12 mice. As we have previously described, by Western blot analyses, we have further confirmed that FKBP12 is overexpressed in αMyHC-FKBP12 atria ~11-fold compared with nontransgenic (NTG) controls (Fig. 1). Seven αMyHC-FKBP12 and eight NTG control mice were subjected to radiotelemetric ECG recordings. Paroxysmal AF was documented during telemetric monitoring in four of seven αMyHC-FKBP12 mice (Fig. 2, *A* and *B*) but in none of eight NTG control mice ($P = 0.03$). The rhythm shown in Fig. 2*A* demonstrates that the initial phase of the tachycardia (*line 2*) consists of slower but irregular rhythm, with variable P waves. This initial phase of rhythm might be consistent with multifocal atrial tachycardia. The rhythm then degenerated into AF with more rapid atrioventricular conduction (*line 3*). To better understand this arrhythmogenic phenotype, we performed electrophysiological experiments using Langendorff-perfused hearts (Fig. 2*C*). Spontaneous AF was observed in three of eight αMyHC-FKBP12 hearts during the electrophysiological experiments but in none of eight NTG hearts. There were prolonged sinus pauses after cessation of paroxysmal AF, resembling tachybrady syndrome in humans. As shown in our previous work (17), the heart rate of αMyHC-FKBP12 mice was 222 ± 35 beats/min, which was significantly slower compared with that measured in NTG control mice (472 ± 29 beats/min).

Impaired atrial conduction and prolonged APD in αMyHC-FKBP12 mice. To determine the underlying electrophysiological mechanism for the occurrence of AF in FKBP12 transgenic mice, we first measured conduction velocity in atria using the optical mapping technique. The conduction velocity of the atria was significantly decreased in αMyHC-FKBP12 hearts ($n = 8$) compared with NTG littermate control hearts ($n = 6$, 0.22 ± 0.03 vs. 0.71 ± 0.08 m/s, $P < 0.05$; Fig. 3, *A* and *B*). We further compared the APD of isolated single left atrial cells from NTG and αMyHC-FKBP12 hearts using the whole cell patch-clamp technique. We found that mean APD at 50% repolarization increased from 6.58 ± 0.61 ms in NTG hearts to 23.9 ± 5.4 ms in αMyHC-FKBP12 hearts ($P < 0.05$; Fig. 3, *C* and *D*); however, mean APD at 50−70% and 90% repolarization was not significantly different (Fig. 3, *E* and *F*). The mean *phase 0* overshoot of the AP decreased from 42.8 ± 1.7 mV in NTG hearts to 16.9 ± 3.4 mV in αMyHC-FKBP12 hearts ($P < 0.05$; Fig. 3*G*), suggesting that the altered I_{Na} underlies the abnormal cardiac physiology in transgenic mice.

Decreased I_{Na} in atrial myocytes of αMyHC-FKBP12 mice. To determine I_{Na} properties in atrial cells, whole cell I_{Na} was evaluated in αMyHC-FKBP12 and littermate control atrial cardiomyocytes. I_{Na} was elicited during 50-ms square-wave voltage steps to various test potentials ranging from −90 to +30 mV (5-mV increments, holding potential: −100 mV, interpulse interval: 1.0 s) in NTG and αMyHC-FKBP12 atrial cardiomyocytes (Fig. 4*A*). Mean peak I_{Na} density was dramatically reduced in atrial cardiomyocytes from αMyHC-FKBP12 mice ($n = 15$ cells/3 mice) compared with NTG mice ($n = 20$ cells/4 mice, 38.7 ± 5.8 vs. 97.2 ± 5.8 pA/pF, $P < 0.05$; Fig. 4, *B* and *C*), which is consistent with the finding in ventricular cardiomyocytes. The voltage dependence of steady-state inactivation of I_{Na} was shifted toward more positive potentials in αMyHC-FKBP12 cardiomyocytes ($V_{1/2}$: −91.1 ± 2.9 mV in αMyHC-FKBP12 mice vs. −84.4 ± 4.4 mV in NTG mice, $P < 0.05$; Fig. 4*D*), whereas the activation and recovery curves showed no apparent alteration in αMyHC-FKBP12 compared with control atrial cardiomyocytes (Fig. 4, *D* and *E*).

Interestingly, in contrast to our previous observation in transgenic ventricular cardiomyocytes, we did not observe a significant increase of late I_{Na} in atrial cardiomyocytes (not shown), suggesting cell type-specific regulation of I_{Na}. The lack of late I_{Na} may explain the normal APD at 90% repolarization in αMyHC-FKBP12 atrial cardiomyocytes.

L-type Ca^{2+} current and K^+ currents in atrial cardiomyocytes of αMyHC-FKBP12 mice. As APD at 50% repolarization is prolonged, we postulated that other ion currents contributing to repolarization were altered. Thus, we specifically recorded L-type Ca^{2+} current ($I_{Ca,L}$) and K^+ currents. Interestingly, in contrast to the reduced peak $I_{Ca,L}$ density in αMyHC-FKBP12 ventricular cardiomyocytes, mean peak $I_{Ca,L}$ density was found to be significantly increased in αMyHC-FKBP12 atrial cardiomyocytes (13 cells/4 mice) compared with NTG atrial cardiomyocytes (10 cells/4 mice, 18.4 ± 1.9 vs. 10.1 ± 0.7 pA/pF, $P < 0.05$; Fig. 5, *A–C*). $I_{Ca.L}$ properties, including activation, inactivation, and recovery from inactivation, showed no apparent alterations (Fig. 5, *D* and *E*, and Table 1). We also evaluated transient outward K^+ current (I_{to}), sustained K^+ current (I_{Ksus}), and inwardly rectifying K^+ current (I_{K1}) in αMyHC-FKBP12 atrial cardiomyocytes. FKBP12 overexpression produced no significant influence on I_{to}, I_{Ksus}, and I_{K1} densities (Fig. 6).

Expression of $Na_v1.5$ and $Ca_v1.2$ in atria of αMyHC-FKBP12 mice. To further evaluate the molecular basis for reduced I_{Na} and increased $I_{Ca,L}$, we examined the level of $Na_v1.5$ (the pore-forming subunit of the major cardiac voltage-gate Na^+ channel) and $Ca_v1.2$ (the pore-forming subunit of cardiac L-type Ca^{2+} channels) by Western blot analysis. Consistent with the decreased peak I_{Na} density, we found that the protein level of $Na_v1.5$ in αMyHC-FKBP12 atria was reduced by 7.7-fold compared with NTG atria ($P < 0.05$; Fig. 7*A*). Interestingly, in contrast to the normal expression level in ventricles, the $Ca_v1.2$ protein expression level showed a significant 2.5-fold increase in αMyHC-FKBP12 atria compared with NTG control atria (Fig. 7*B*).

Altered atrial histology in αMyHC-FKBP12 hearts. We further evaluated the atrial anatomy of αMyHC-FKBP12 hearts. We not only confirmed that both atria of αMyHC-FKBP12 hearts were enlarged but also found that both atria of αMyHC-FKBP12 hearts were significantly more fibrotic compared with NTG littermate control hearts (Fig. 8, *A* and *B*) Picrosirius red staining showed that the amount of fibrosis was dramatically increased in the atria of αMyHC-FKBP12 mice (8 wk old) compared with NTG littermates (Fig. 8, *C–F*). The fibrotic areas were 0.42 ± 0.45% in NTG littermates and 2.17 ± 0.98% in αMyHC-FKBP12 mice ($P < 0.05$).

DISCUSSION

FKBP12 is a cardiac enriched protein. We have previously shown that FKBP12 plays an important role in cardiac development (27) and ventricular conduction defects (17). In this study, we found that FKBP12 overexpression also causes changes of atrial electrophysiology and facilitates the development of spontaneous AF. The most prominent changes of ion channel expression include reduced peak I_{Na} and increased peak $I_{Ca,L}$. In contrast to the findings in ventricular cardiomyocytes, late I_{Na} was not increased in atrial cardiomyocytes. These findings show that chronic FKBP12 overexpression has differential effects on the electrophysiological characteristics of atrial and ventricular cardiomyocytes.

Changes of I_{Na}. Functional and anatomic reentry is an important mechanism of AF. Either increased atrial size or shortened impulse wavelength by decreased conduction velocity and/or refractory period facilitates the formation of multiple wavelets and occurrence of AF (2). In the present study, we found that the atria were enlarged and atrial conduction velocity in αMyHC-FKBP12-overexpressing mice was slower than in NTG control mice. A major determinant of electrical conduction in the atria is the magnitude of Na^+ influx through voltage-gated Na^+ channels during the initial fast membrane depolarization (14). Consistent with a

reduced conduction velocity, we found that there was reduced peak I_{Na} and downregulation of $Na_v1.5$ protein in transgenic mice compared with NTG control mice. The increased availability of the Na^+ channel in αMyHC-FKBP12 transgenic mice resulting from a positive shift of the inactivation curve was apparently insufficient to compensate for the reduction in peak I_{Na}. Moreover, the positive shift of the I_{Na} inactivation curve causes an increase in steady-state ("window") current, which may contribute to the APD prolongation. I_{Na} was reduced in atrial cardiomyocytes from patients with AF (28) and from dogs with pacing-induced AF (35). Watanabe et al. (33) established a knockin mouse model carrying the human D1275N-SCN5A mutation. They observed I_{Na} reduction, conduction slowing, and AF occurrence. These findings provide direct evidence for the causal role of reduced Na^+ channel function and the mechanisms of AF.

Although we (17) and others (22, 30) showed that simultaneous increment of late I_{Na} may accompany reduced peak I_{Na}, no increase of late I_{Na} density was observed in atrial cardiomyocytes of αMyHC-FKBP12 mice. Previous studies have documented different expression of ion channel genes and differential regulation of channels in atrial and ventricular cardiomyocytes (21), which may lead to significant differences of the biophysical characteristics of I_{Na}. For example, the half-inactivation voltage of I_{Na} was more negative in atrial versus ventricular cardiomyocytes (4, 15). Recovery of I_{Na} from inactivation was slower in atrial cardiomyocytes than in ventricular cardiomyocytes, whereas the development of resting state inactivation was more rapid in atrial cardiomyocytes than in ventricular cardiomyocytes (15). These biophysical differences of atrial and ventricular I_{Na} may in part account for the differential effects of FKBP12 overexpression on late I_{Na}.

Increased Ca^{2+} current. An unexpected finding in this study was that $I_{Ca,L}$ is increased in atrial cardiomyocytes of transgenic mice compared with NTG control mice. Ca^{2+} influx during the AP plateau is important in determining APD. An increase of $I_{Ca,L}$, an inward current, tends to keep the cell depolarized and prolongs APD (20). Ca^{2+} also activates cardiac RyR2 to release Ca^{2+} from the sarcoplasmic reticulum. The latter process may also be in part controlled by FKBP12 (10, 26). In the present study, we recorded a significant increase of $I_{Ca,L}$ density in atrial cardiomyocytes of αMyHC-FKBP12 mice, with no channel kinetic alterations. This augmentation of $I_{Ca,L}$ can be explained by the concurrent upregulation of $Ca_v1.2$, the pore-forming protein of the Ca^{2+} channel. We think that one possible mechanism of $Ca_v1.2$ upregulation is that FKBP12 directly upregulates $Ca_v1.2$ production. However, there are no data to support this hypothesis. An alternative explanation is a secondary event due to the atrial enlargement based on the following: *1*) short-term overexpression of FKBP12 in rabbit ventricular myocytes by adenoviral system produced no changes in $I_{Ca,L}$ (26); *2*) acute treatment of FK506 did not alter $I_{Ca,L}$ densities and *I-V* relationships in either rabbit, rat, or mouse ventricular cardiomyocytes (19, 29, 34); and *3*) $I_{Ca,L}$ did not change in ventricular cardiomyocytes of αMyHC-FKBP12 mice from the same line as used in the present study (17). Because the latter study recorded $I_{Ca,L}$ at room temperature while the present study recorded $I_{Ca,L}$ at 37°C, it is possible that the different recording temperatures played a role in these findings. Therefore, we repeated the patch-clamp experiments of ventricular cardiomyocytes at 37°C. The results showed no change of $I_{Ca,L}$ in αMyHC-FKBP12 ventricular cardiomyocytes (not shown) (4). $I_{Ca,L}$ is often increased in models of mild to moderate hypertrophy (1). The αMyHC-FKBP12 mouse has significantly enlarged atria but not ventricles. The differential expression of $I_{Ca,L}$ in atrial and ventricular cardiomyocytes may be due to the greater pathological effects of FKBP12 overexpression on the atria than ventricles. However, the mechanism by which FKBP12 induced atrial but not ventricular enlargement remains unclear. The relationship between atrial enlargement and $I_{Ca,L}$ upregulation is also unclear.

Interstitial fibrosis. Interstitial fibrosis is an important contributor to the AF substrate and may affect atrial conduction (20). We found that there was significantly more atrial fibrosis in αMyHC-FKBP12 mice than in NTG mice. The increased fibrosis may contribute to the mechanisms of AF. A direct effect of FKBP12 is

unlikely as the cause of atrial fibrosis, because FKBP12 inhibits the transforming growth factor-β type I receptors (32). Because previous studies have documented increased fibrosis in mice with SCN5A mutation (24, 31), it is possible that reduced I_{Na} and $Na_v1.5$ in FKBP12 transgenic mice caused increased fibrosis in the atria. The molecular mechanisms by which FKBP12 regulates $Na_v1.5$ biochemically remain undetermined.

Conclusions. In summary, we found that FKBP12 overexpression in the mouse heart caused enlarged atria, atrial fibrosis, reduced peak I_{Na} density, and enhanced peak $I_{Ca,L}$ density in atrial cardiomyocytes, which, in turn, decreased atrial conduction velocity and prolonged APD. These morphological and electrical alterations facilitated the development of spontaneous AF.

GRANTS

This work was supported in part by National Heart, Lung, and Blood Institute Grants P01-HL-78931, R01-HL-71140, and R21-HL-106554 (to P.-S. Shen) and R01-HL-81092 and P01-HL-85098 (to W. Shou); Medtronic-Zipes Endowment (to P.-S. Chen); Riley Children Foundation (to W. Shou); and National Natural Science Foundation of China Grant 81573431 (to B. Li) and 81470463 (to Z. Pan).

DISCLOSURES

Medtronic, St. Jude, Cryocath, and Cyberonics donated research equipment used in this study. P.-S. Chen is a consultant to Cyberonics.

AUTHOR CONTRIBUTIONS

P.-S.C., W.S., and B.-Y.L. conceived and designed research; Z.P., P.-C.C., Y.L., J.L., M.M., M.H., and H.C. performed experiments; Z.P., T.A., P.-C.C., Y.L., M.M., M.H., D.X., H.C., P.-S.C., W.S., and B.-Y.L. analyzed data; Z.P., J.L., M.M., M.C.F., S.-F.L., P.-S.C., W.S., and B.-Y.L. interpreted results of experiments; Z.P. prepared figures; Z.P. drafted manuscript; Z.P., T.A., P.-C.C., M.M., M.C.F., M.R., S.-F.L., D.X., H.C., P.-S.C., W.S., and B.-Y.L. edited and revised manuscript; and Z.P., T.A., P.-C.C., Y.L., J.L., M.M., M.H., M.C.F., M.R., S.-F.L., D.X., H.C., P.-S.C., W.S., and B.-Y.L. approved final version of manuscript.

ACKNOWLEDGMENTS

We thank Nicole Courtney, Lei Lin, and Jessica Warfel for assistance. We also thank Dr. Peter Mohler (Ohio State University) for providing the antibody to $Na_v1.5$.

REFERENCES

1. Armoundas AA, Wu R, Juang G, Marbán E, Tomaselli GF. Electrical and structural remodeling of the failing ventricle. Pharmacol Ther 92: 213–230, 2001. doi:10.1016/S0163-7258(01)00171-1. [PubMed: 11916538] [CrossRef: 10.1016/S0163-7258(01)00171-1]

2. Benjamin EJ, Chen PS, Bild DE, Mascette AM, Albert CM, Alonso A, Calkins H, Connolly SJ, Curtis AB, Darbar D, Ellinor PT, Go AS, Goldschlager NF, Heckbert SR, Jalife J, Kerr CR, Levy D, Lloyd-Jones DM, Massie BM, Nattel S, Olgin JE, Packer DL, Po SS, Tsang TS, Van Wagoner DR, Waldo AL, Wyse DG. Prevention of atrial fibrillation: report from a National Heart, Lung, and Blood Institute workshop. Circulation 119: 606–618, 2009. doi:10.1161/CIRCULATIONAHA.108.825380. [PMCID: PMC2635942] [PubMed: 19188521] [CrossRef: 10.1161/CIRCULATIONAHA.108.825380]

3. Brugada J, Brugada R, Brugada P. Channelopathies: a new category of diseases causing sudden death [in English]. Herz 32: 185–191, 2007. doi:10.1007/s00059-007-2976-1. [PubMed: 17497250] [CrossRef:

10.1007/s00059-007-2976-1]

4. Burashnikov A, Di Diego JM, Zygmunt AC, Belardinelli L, Antzelevitch C. Atrium-selective sodium channel block as a strategy for suppression of atrial fibrillation: differences in sodium channel inactivation between atria and ventricles and the role of ranolazine. Circulation 116: 1449–1457, 2007. doi:10.1161/CIRCULATIONAHA.107.704890. [PMCID: PMC2566303] [PubMed: 17785620] [CrossRef: 10.1161/CIRCULATIONAHA.107.704890]

5. Chen LY, Ballew JD, Herron KJ, Rodeheffer RJ, Olson TM. A common polymorphism in *SCN5A* is associated with lone atrial fibrillation. Clin Pharmacol Ther 81: 35–41, 2007. doi:10.1038/sj.clpt.6100016. [PMCID: PMC1933493] [PubMed: 17185997] [CrossRef: 10.1038/sj.clpt.6100016]

6. Cox TH, Baillie GM, Baliga P. Bradycardia associated with intravenous administration of tacrolimus in a liver transplant recipient. Pharmacotherapy 17: 1328–1330, 1997. [PubMed: 9399620]

7. Darbar D, Kannankeril PJ, Donahue BS, Kucera G, Stubblefield T, Haines JL, George AL Jr, Roden DM. Cardiac sodium channel (*SCN5A*) variants associated with atrial fibrillation. Circulation 117: 1927–1935, 2008. doi:10.1161/CIRCULATIONAHA.107.757955. [PMCID: PMC2365761] [PubMed: 18378609] [CrossRef: 10.1161/CIRCULATIONAHA.107.757955]

8. Domínguez JN, de la Rosa A, Navarro F, Franco D, Aránega AE. Tissue distribution and subcellular localization of the cardiac sodium channel during mouse heart development. Cardiovasc Res 78: 45–52, 2008. doi:10.1093/cvr/cvm118. [PubMed: 18178574] [CrossRef: 10.1093/cvr/cvm118]

9. Ellinor PT, Nam EG, Shea MA, Milan DJ, Ruskin JN, MacRae CA. Cardiac sodium channel mutation in atrial fibrillation. Heart Rhythm 5: 99–105, 2008. doi:10.1016/j.hrthm.2007.09.015. [PubMed: 18088563] [CrossRef: 10.1016/j.hrthm.2007.09.015]

10. Galfré E, Pitt SJ, Venturi E, Sitsapesan M, Zaccai NR, Tsaneva-Atanasova K, O'Neill S, Sitsapesan R. FKBP12 activates the cardiac ryanodine receptor Ca^{2+}-release channel and is antagonised by FKBP12.6. PLoS One 7: e31956, 2012. doi:10.1371/journal.pone.0031956. [PMCID: PMC3283708] [PubMed: 22363773] [CrossRef: 10.1371/journal.pone.0031956]

11. Heeringa J, van der Kuip DA, Hofman A, Kors JA, van Herpen G, Stricker BH, Stijnen T, Lip GY, Witteman JC. Prevalence, incidence and lifetime risk of atrial fibrillation: the Rotterdam study. Eur Heart J 27: 949–953, 2006. doi:10.1093/eurheartj/ehi825. [PubMed: 16527828] [CrossRef: 10.1093/eurheartj/ehi825]

12. Hodak SP, Moubarak JB, Rodriguez I, Gelfand MC, Alijani MR, Tracy CM. QT prolongation and near fatal cardiac arrhythmia after intravenous tacrolimus administration: a case report. Transplantation 66: 535–537, 1998. doi:10.1097/00007890-199808270-00021. [PubMed: 9734501] [CrossRef: 10.1097/00007890-199808270-00021]

13. Kim MH, Johnston SS, Chu BC, Dalal MR, Schulman KL. Estimation of total incremental health care costs in patients with atrial fibrillation in the United States. Circ Cardiovasc Qual Outcomes 4: 313–320, 2011. doi:10.1161/CIRCOUTCOMES.110.958165. [PubMed: 21540439] [CrossRef: 10.1161/CIRCOUTCOMES.110.958165]

14. Kléber AG, Rudy Y. Basic mechanisms of cardiac impulse propagation and associated arrhythmias. Physiol Rev 84: 431–488, 2004. doi:10.1152/physrev.00025.2003. [PubMed: 15044680] [CrossRef: 10.1152/physrev.00025.2003]

15. Li GR, Lau CP, Shrier A. Heterogeneity of sodium current in atrial vs epicardial ventricular myocytes of adult guinea pig hearts. J Mol Cell Cardiol 34: 1185–1194, 2002. doi:10.1006/jmcc.2002.2053.

[PubMed: 12392892] [CrossRef: 10.1006/jmcc.2002.2053]

16. Lu Y, Zhang Y, Wang N, Pan Z, Gao X, Zhang F, Zhang Y, Shan H, Luo X, Bai Y, Sun L, Song W, Xu C, Wang Z, Yang B. MicroRNA-328 contributes to adverse electrical remodeling in atrial fibrillation. Circulation 122: 2378–2387, 2010. doi:10.1161/CIRCULATIONAHA.110.958967. [PubMed: 21098446] [CrossRef: 10.1161/CIRCULATIONAHA.110.958967]

17. Maruyama M, Li BY, Chen H, Xu X, Song LS, Guatimosim S, Zhu W, Yong W, Zhang W, Bu G, Lin SF, Fishbein MC, Lederer WJ, Schild JH, Field LJ, Rubart M, Chen PS, Shou W. FKBP12 is a critical regulator of the heart rhythm and the cardiac voltage-gated sodium current in mice. Circ Res 108: 1042–1052, 2011. doi:10.1161/CIRCRESAHA.110.237867. [PMCID: PMC3092589] [PubMed: 21372286] [CrossRef: 10.1161/CIRCRESAHA.110.237867]

18. Marx SO, Ondrias K, Marks AR. Coupled gating between individual skeletal muscle Ca2+ release channels (ryanodine receptors). Science 281: 818–821, 1998. doi:10.1126/science.281.5378.818. [PubMed: 9694652] [CrossRef: 10.1126/science.281.5378.818]

19. McCall E, Li L, Satoh H, Shannon TR, Blatter LA, Bers DM. Effects of FK-506 on contraction and Ca^{2+} transients in rat cardiac myocytes. Circ Res 79: 1110–1121, 1996. doi:10.1161/01.RES.79.6.1110. [PubMed: 8943949] [CrossRef: 10.1161/01.RES.79.6.1110]

20. Nattel S, Burstein B, Dobrev D. Atrial remodeling and atrial fibrillation: mechanisms and implications. Circ Arrhythm Electrophysiol 1: 62–73, 2008. doi:10.1161/CIRCEP.107.754564. [PubMed: 19808395] [CrossRef: 10.1161/CIRCEP.107.754564]

21. Ng SY, Wong CK, Tsang SY. Differential gene expressions in atrial and ventricular myocytes: insights into the road of applying embryonic stem cell-derived cardiomyocytes for future therapies. Am J Physiol Cell Physiol 299: C1234–C1249, 2010. doi:10.1152/ajpcell.00402.2009. [PubMed: 20844252] [CrossRef: 10.1152/ajpcell.00402.2009]

22. Remme CA, Verkerk AO, Nuyens D, van Ginneken AC, van Brunschot S, Belterman CN, Wilders R, van Roon MA, Tan HL, Wilde AA, Carmeliet P, de Bakker JM, Veldkamp MW, Bezzina CR. Overlap syndrome of cardiac sodium channel disease in mice carrying the equivalent mutation of human *SCN5A*-1795insD. Circulation 114: 2584–2594, 2006. doi:10.1161/CIRCULATIONAHA.106.653949. [PubMed: 17145985] [CrossRef: 10.1161/CIRCULATIONAHA.106.653949]

23. Remme CA, Wilde AA, Bezzina CR. Cardiac sodium channel overlap syndromes: different faces of SCN5A mutations. Trends Cardiovasc Med 18: 78–87, 2008. doi:10.1016/j.tcm.2008.01.002. [PubMed: 18436145] [CrossRef: 10.1016/j.tcm.2008.01.002]

24. Royer A, van Veen TA, Le Bouter S, Marionneau C, Griol-Charhbili V, Léoni AL, Steenman M, van Rijen HV, Demolombe S, Goddard CA, Richer C, Escoubet B, Jarry-Guichard T, Colledge WH, Gros D, de Bakker JM, Grace AA, Escande D, Charpentier F. Mouse model of *SCN5A*-linked hereditary Lenègre's disease: age-related conduction slowing and myocardial fibrosis. Circulation 111: 1738–1746, 2005. doi:10.1161/01.CIR.0000160853.19867.61. [PubMed: 15809371] [CrossRef: 10.1161/01.CIR.0000160853.19867.61]

25. Sawabe T, Mizuno S, Gondo H, Maruyama T, Niho Y. Sinus arrest during tacrolimus (FK506) and digitalis treatment in a bone marrow transplant recipient. Transplantation 64: 182–183, 1997. doi:10.1097/00007890-199707150-00035. [PubMed: 9233725] [CrossRef: 10.1097/00007890-199707150-00035]

26. Seidler T, Loughrey CM, Zibrova D, Kettlewell S, Teucher N, Kögler H, Hasenfuss G, Smith GL. Overexpression of FK-506 binding protein 12.0 modulates excitation contraction coupling in adult rabbit

ventricular cardiomyocytes. Circ Res 101: 1020–1029, 2007. doi:10.1161/CIRCRESAHA.107.154609. [PubMed: 17872463] [CrossRef: 10.1161/CIRCRESAHA.107.154609]

27. Shou W, Aghdasi B, Armstrong DL, Guo Q, Bao S, Charng MJ, Mathews LM, Schneider MD, Hamilton SL, Matzuk MM. Cardiac defects and altered ryanodine receptor function in mice lacking FKBP12. Nature 391: 489–492, 1998. doi:10.1038/35146. [PubMed: 9461216] [CrossRef: 10.1038/35146]

28. Sossalla S, Kallmeyer B, Wagner S, Mazur M, Maurer U, Toischer K, Schmitto JD, Seipelt R, Schöndube FA, Hasenfuss G, Belardinelli L, Maier LS. Altered Na^+ currents in atrial fibrillation effects of ranolazine on arrhythmias and contractility in human atrial myocardium. J Am Coll Cardiol 55: 2330–2342, 2010. doi:10.1016/j.jacc.2009.12.055. [PubMed: 20488304] [CrossRef: 10.1016/j.jacc.2009.12.055]

29. Su Z, Sugishita K, Li F, Ritter M, Barry WH. Effects of FK506 on $[Ca^{2+}]_i$ differ in mouse and rabbit ventricular myocytes. J Pharmacol Exp Ther 304: 334–341, 2003. doi:10.1124/jpet.102.041210. [PubMed: 12490609] [CrossRef: 10.1124/jpet.102.041210]

30. Tan BH, Iturralde-Torres P, Medeiros-Domingo A, Nava S, Tester DJ, Valdivia CR, Tusié-Luna T, Ackerman MJ, Makielski JC. A novel C-terminal truncation *SCN5A* mutation from a patient with sick sinus syndrome, conduction disorder and ventricular tachycardia. Cardiovasc Res 76: 409–417, 2007. doi:10.1016/j.cardiores.2007.08.006. [PMCID: PMC2100438] [PubMed: 17897635] [CrossRef: 10.1016/j.cardiores.2007.08.006]

31. van Veen TA, Stein M, Royer A, Le Quang K, Charpentier F, Colledge WH, Huang CL, Wilders R, Grace AA, Escande D, de Bakker JM, van Rijen HV. Impaired impulse propagation in *Scn5a*-knockout mice: combined contribution of excitability, connexin expression, and tissue architecture in relation to aging. Circulation 112: 1927–1935, 2005. doi:10.1161/CIRCULATIONAHA.105.539072. [PubMed: 16172272] [CrossRef: 10.1161/CIRCULATIONAHA.105.539072]

32. Wang T, Li BY, Danielson PD, Shah PC, Rockwell S, Lechleider RJ, Martin J, Manganaro T, Donahoe PK. The immunophilin FKBP12 functions as a common inhibitor of the TGFβ family type I receptors. Cell 86: 435–444, 1996. doi:10.1016/S0092-8674(00)80116-6. [PubMed: 8756725] [CrossRef: 10.1016/S0092-8674(00)80116-6]

33. Watanabe H, Yang T, Stroud DM, Lowe JS, Harris L, Atack TC, Wang DW, Hipkens SB, Leake B, Hall L, Kupershmidt S, Chopra N, Magnuson MA, Tanabe N, Knollmann BC, George AL Jr, Roden DM. Striking in vivo phenotype of a disease-associated human *SCN5A* mutation producing minimal changes in vitro. Circulation 124: 1001–1011, 2011. doi:10.1161/CIRCULATIONAHA.110.987248. [PMCID: PMC3297976] [PubMed: 21824921] [CrossRef: 10.1161/CIRCULATIONAHA.110.987248]

34. Xiao RP, Valdivia HH, Bogdanov K, Valdivia C, Lakatta EG, Cheng H. The immunophilin FK506-binding protein modulates Ca^{2+} release channel closure in rat heart. J Physiol 500: 343–354, 1997. doi:10.1113/jphysiol.1997.sp022025. [PMCID: PMC1159388] [PubMed: 9147322] [CrossRef: 10.1113/jphysiol.1997.sp022025]

35. Yagi T, Pu J, Chandra P, Hara M, Danilo P Jr, Rosen MR, Boyden PA. Density and function of inward currents in right atrial cells from chronically fibrillating canine atria. Cardiovasc Res 54: 405–415, 2002. doi:10.1016/S0008-6363(02)00279-1. [PubMed: 12062345] [CrossRef: 10.1016/S0008-6363(02)00279-1]

Figures and Tables

Fig. 1.

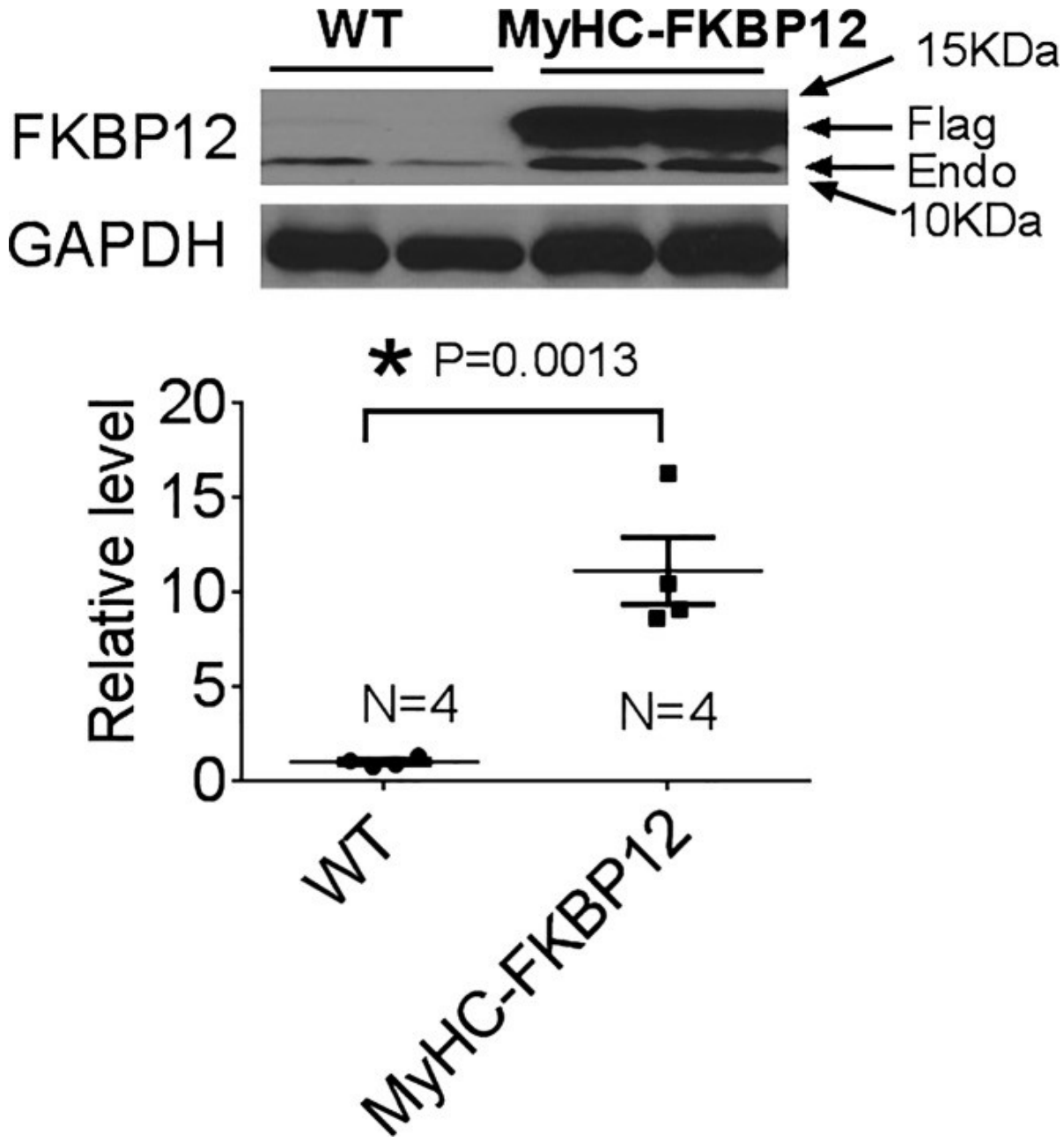

Open in a separate window

Protein level of FK506-binding protein 12 (FKBP12) in the atria of FKBP12 transgenic (αMyHC-FKBP12) mice. Endogenous FKBP12 (Endo) and overexpressed transgenic flag-FKBP12 (Flag) are indicated by arrows. WT, wild type. Data are expressed as means ± SE; $n = 4$. *$P < 0.05$ vs. nontransgenic (NTG) mice.

Fig. 2.

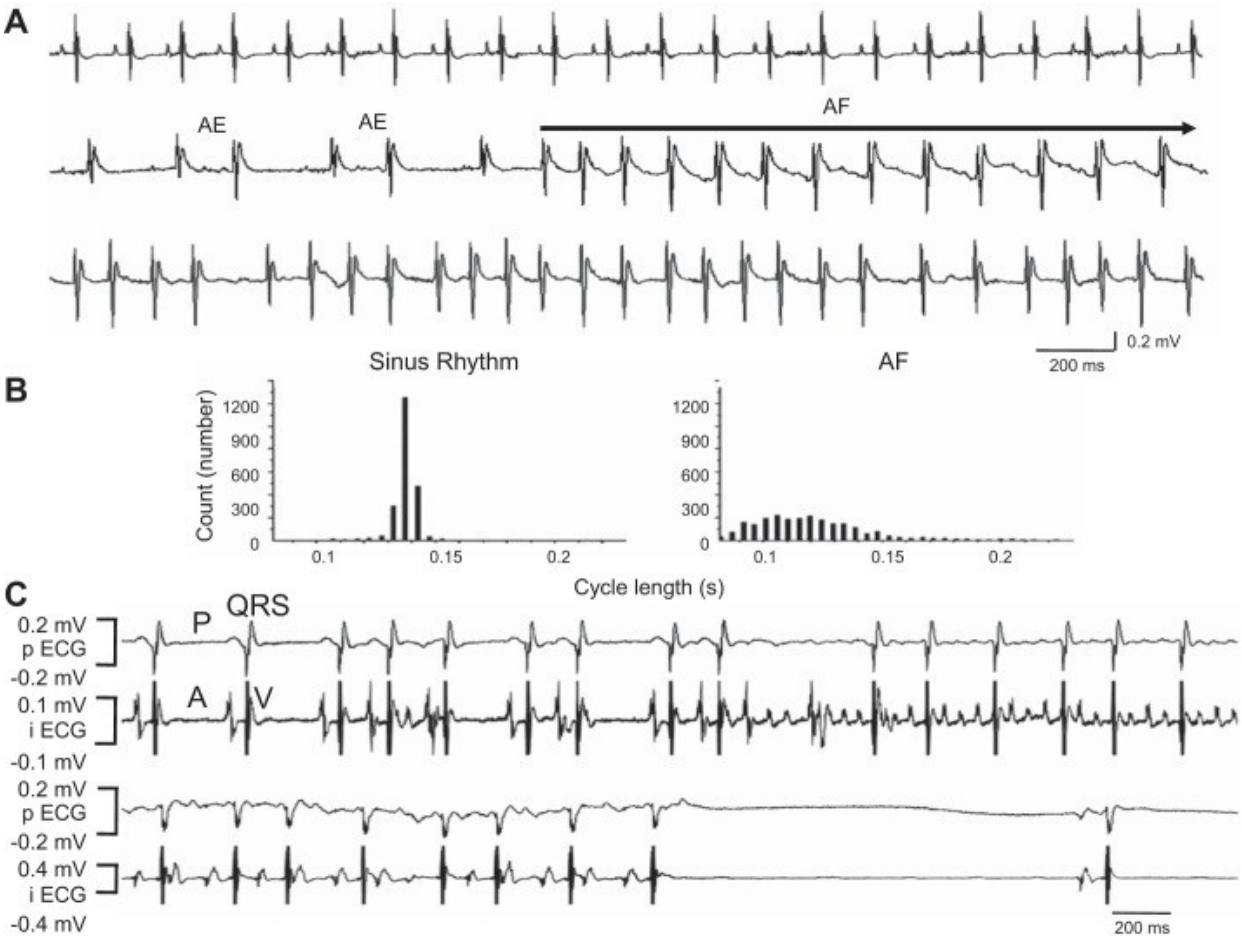

Atrial fibrillation (AF) in FK506-binding protein 12 transgenic (αMyHC-FKBP12) mice. *A*: paroxysmal AF documented by ambulatory ECG. *B*: the diagnosis of AF was supported by the absence of P waves despite the presence of clear P waves during sinus rhythm and irregular rhythm, which was evident in the 5-min cycle length histogram. *C*: AF occurred spontaneously during the electrophysiological experiment (*top* traces). Note that the termination of AF was followed by prolonged sinus pause (*bottom* traces), suggesting abnormal sinus node function. AE, atrial ectopy; pECG, pseudo ECG; iECG, intracardiac electrograms.

Fig. 3.

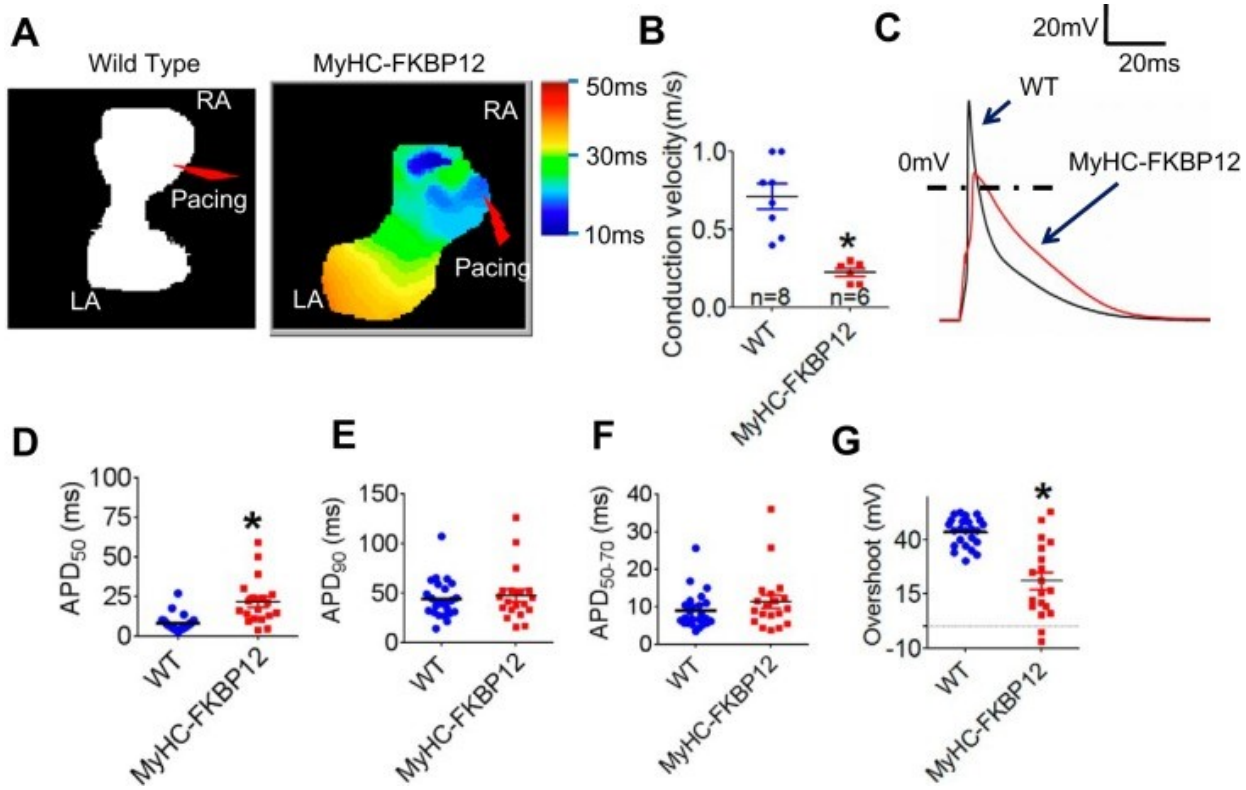

Conduction velocity (CV) and action potential (AP) duration (APD) in the atria of FK506-binding protein 12 transgenic (αMyHC-FKBP12) mice. *A*: representative pictures of AP propagation in the atria by optical mapping. Scale bar = 2 mm. *B*: comparison of atrial CV between αMyHC-FKBP12 and nontransgenic (NTG) control mice. *C*: representative AP traces in single atrial myocytes. *D–G*: comparison of APD at 50%, 90%, and 50-70% repolarization (APD_{50}, APD_{90}, and $APD_{50–70}$, respectively) and the AP overshoot between atrial myocytes from αMyHC-FKBP12 (n = 19 cells/4 mice) and NTG control mice (n = 24 cells/4 mice). WT, wild type. Data are expressed as means ± SE. *$P < 0.05$ vs. NTG mice.

Fig. 4.

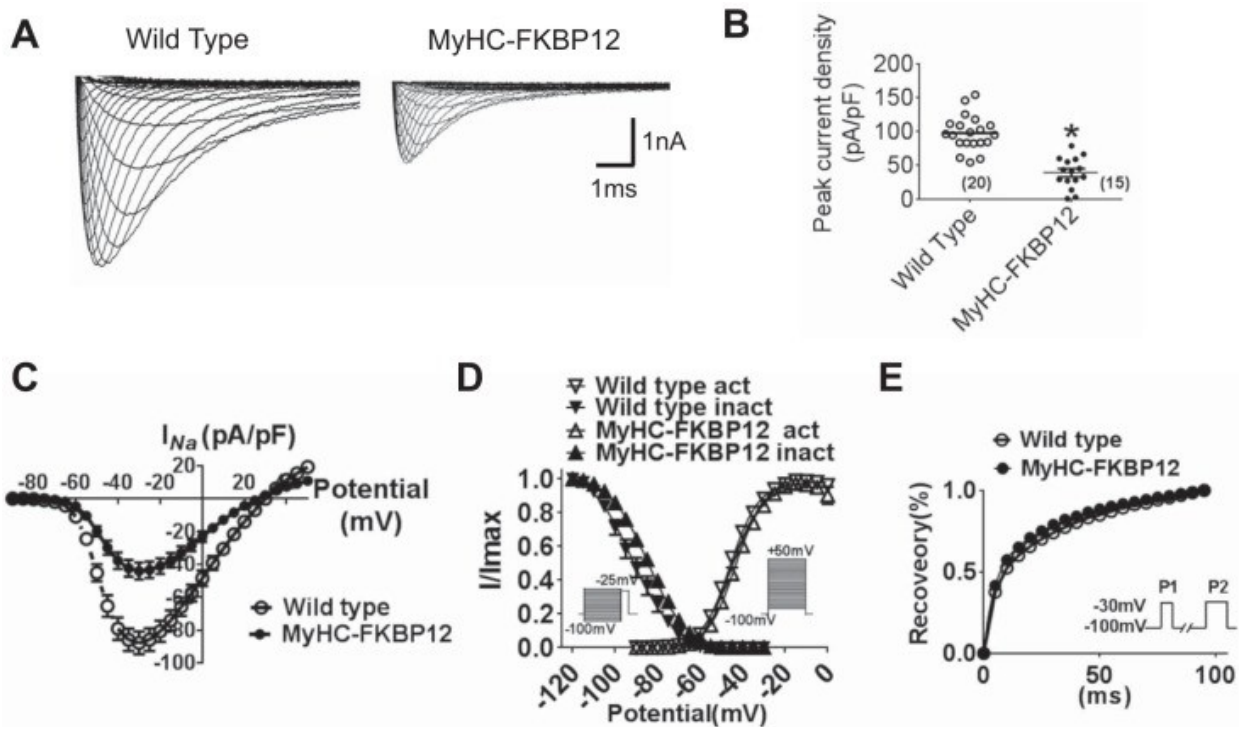

Analysis of Na^+ currents (I_{Na}) of isolated atrial cardiomyocytes in nontransgenic (NTG) and FK506-binding protein 12 transgenic (αMyHC-FKBP12) mice. *A*: representative tracings of total I_{Na}. *B*: peak I_{Na} density from NTG (n = 20 cells/4 mice) and αMyHC-FKBP12 (n = 15 cells/4 mice) atrial myocytes. *C*: current-voltage (*I-V*) relationship (*I-V* curve) for peak I_{Na} density. *D*: voltage dependence of the steady-state activation and inactivation for I_{Na}. For activation, the cell was held at −100 mV and depolarized for 50 ms to potentials between −90 and +10 mV in 5-mV increments. The interpulse interval was 1 s. For inactivation, the cell was held at −100 mV, and 1-s preconditioning pulses to potentials between −120 and −30 mV in 5-mV increments were applied followed by 40-ms test pulses to −25 mV. The interpulse interval was 3 s. *E*: time course of I_{Na} recovery from inactivation. Recovery was recorded by depolarizing the cell to −30 mV from the holding potential of −100 mV for 300 ms (P1) followed by a variable recovery interval and a subsequent −30-mV test pulse (P2). *P < 0.05 vs. NTG mice.

Fig. 5.

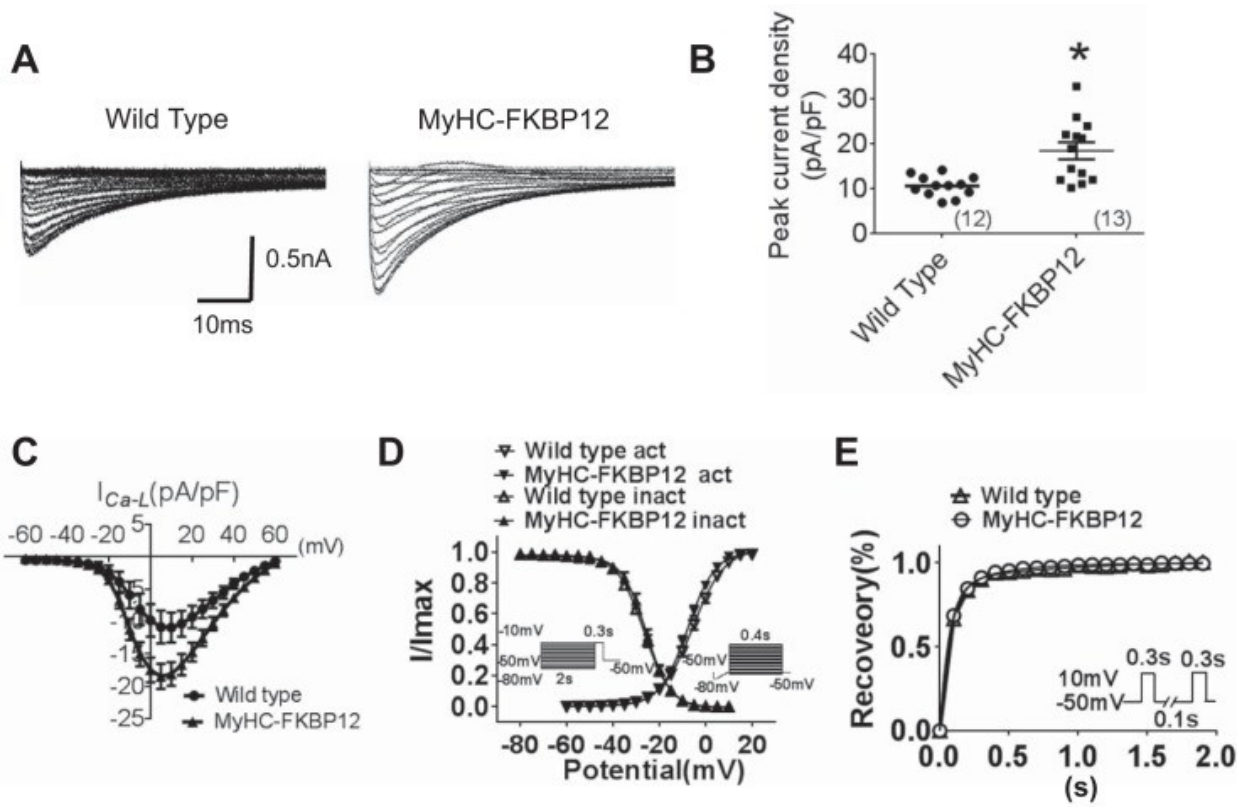

Analysis of cardiac L-type Ca^{2+} currents ($I_{Ca,L}$) from isolated atrial cardiomyocytes in nontransgenic (NTG) and FK506-binding protein 12 transgenic (αMyHC-FKBP12) mice. *A*: representative traces of whole cell $I_{Ca,L}$. *B*: peak $I_{Ca,L}$ density in NTG (n = 12 cells/4 mice) and αMyHC-FKBP12 (n = 13 cells/4 mice) atrial myocytes. *C*: current-voltage (*I-V*) relationship (*I-V* curve) for peak $I_{Ca,L}$. *D*: voltage dependence of the steady-state activation and inactivation for $I_{Ca,L}$. For activation, the cell was held at −50 mV, ramp depolarized from −80 to −50 mV over 100 ms, and step depolarized from −50 to +60 mV with 5-mV increments. The interpulse interval was 2 s. For inactivation, the cell was held at −50 mV, and 2,000-ms preconditioning pulses to potentials from −80 to −10 mV with a 5-mV increment were applied followed by a 300-ms test pulse to −10 mV. *E*: normalized peak $I_{Ca,L}$ (I/I_{max}) for $I_{Ca,L}$ recovery from inactivation. *Inset:* recording protocol. **P* < 0.05 vs. NTG mice.

Table 1.

Properties of I_{Na} and $I_{Ca,L}$ in atrial myocytes

		Nontransgenic	αMyHC-FKBP12
I_{Na}			
	Peak current density, pA/pF	97.2 ± 5.8 (n = 20)	38.7 ± 5.8* (n = 15)
	Activation		
	$V_{½}$, mV	−45.7 ± 1.0 (n = 12)	−43.1 ± 1.2 (n = 13)
	k, mV	6.54 ± 0.23 (n = 12)	6.52 ± 0.38 (n = 13)
	Inactivation		
	$V_{½}$, mV	−92.1 ± 1.03 (n = 11)	−84.4 ± 4.4* (n = 13)
	k, mV	10.16 ± 0.85 (n = 11)	9.27 ± 0.41 (n = 13)
$I_{Ca,L}$			
	Peak current density, pA/pF	10.5 ± 0.66 (n = 12)	18.4 ± 1.91* (n = 13)
	Activation		
	$V_{½}$, mV	−5.44 ± 0.39 (n = 12)	−7.56 ± 0.88 (n = 13)
	k, mV	6.78 ± 0.34 (n = 12)	5.88 ± 0.19 (n = 13)
	Inactivation		
	$V_{½}$, mV	−27.1 ± 0.27 (n = 12)	−25.9 ± 1.02 (n = 12)
	k, mV	5.85 ± 0.23 (n = 12)	4.93 ± 0.20 (n = 12)

Values are means ± SE; n = number of cells from 4 mice. I_{Na}, Na^+ current; $I_{Ca,L}$, L-type Ca^{2+} current; αMyHC-FKBP12, FK506-binding protein 12 transgenic mice; $V_{½}$, midpoint voltage of maximal conductance/currents; k, slope factor.

*$P < 0.05$ vs. nontransgenic mice.

Fig. 6.

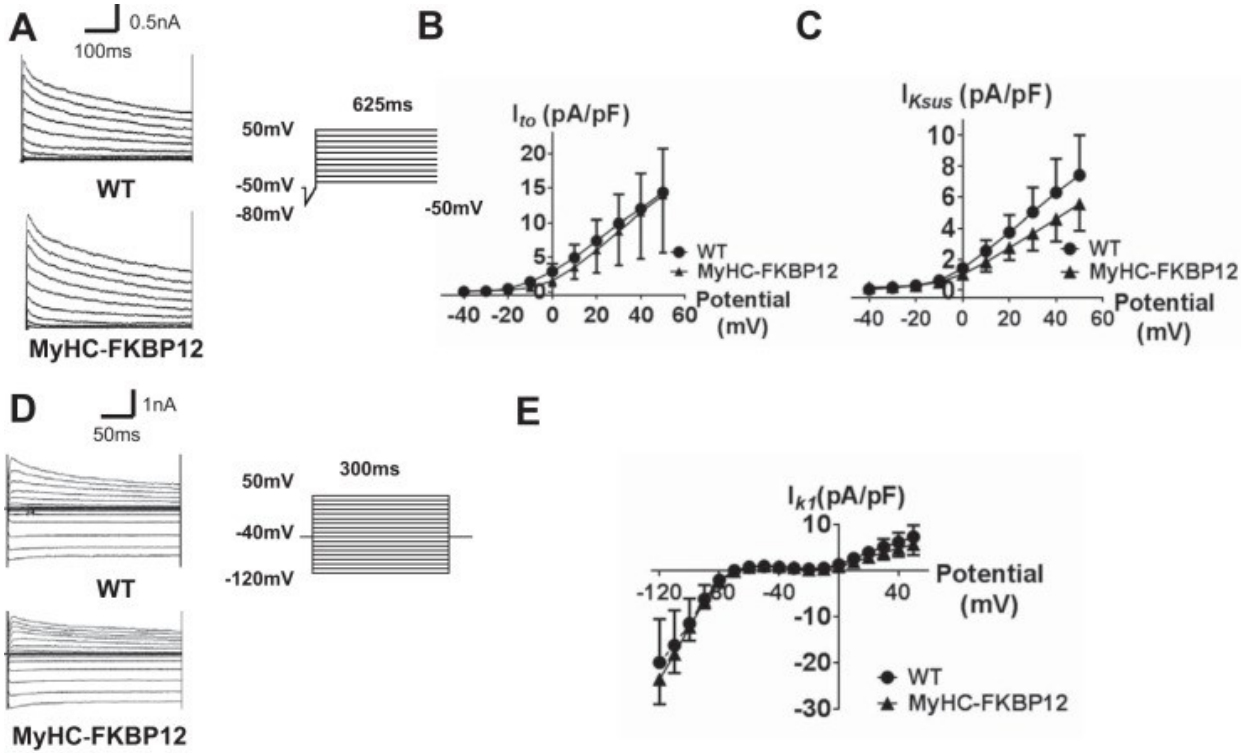

Analysis of cardiac transient outward K^+ currents (I_{to}), sustained K^+ currents (I_{Ksus}), and inward rectifier K^+ currents (I_{K1}) from isolated atrial cardiomyocytes in nontransgenic (NTG) and FK506-binding protein 12 transgenic (αMyHC-FKBP12) mice. *A*: representative I_{to} traces of NTG and αMyHC-FKBP12 myocytes. I_{to} was elicited from a holding potential at −50 mV with a 50-ms ramp from −80 to −40 mV followed by depolarizing pulses from −40 to +50 mV for 625 ms (in 10-mV increments). *B* and *C*: current-voltage (*I-V*) relationship (*I-V* curve) for I_{to} and I_{Ksus}. NTG: n = 21 cells/4 mice and αMyHC-FKBP12: n = 14 cells/4 mice. *D*: representative I_{K1} traces of NTG and αMyHC-FKBP12 myocytes. I_{K1} was elicited by holding the cell at −40 mV followed by 10-mV steps from −120 to 50 mV for 300 ms. *E*: *I-V* curve for I_{K1}. NTG: n = 22 cells/4 mice and αMyHC-FKBP12: n = 18 cells/4 mice. WT, wild type.

Fig. 7.

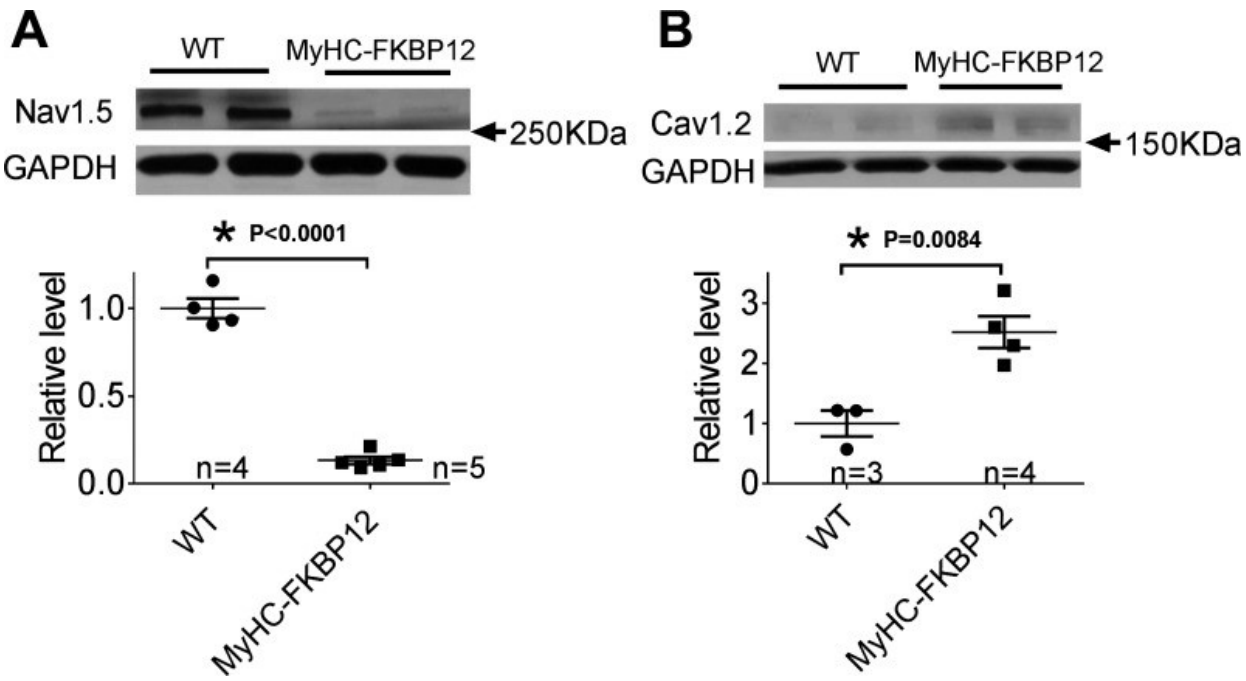

A and *B*: representative Western blots to analyze the expression of $Na_v1.5$ (*A*) and $Ca_v1.2$ (*B*) in the atria of FK506-binding protein 12 transgenic (αMyHC-FKBP12) transgenic mice as evaluated by Western blot analysis. WT, wild type. **P* < 0.05 vs. nontransgenic (NTG) mice.

Fig. 8.

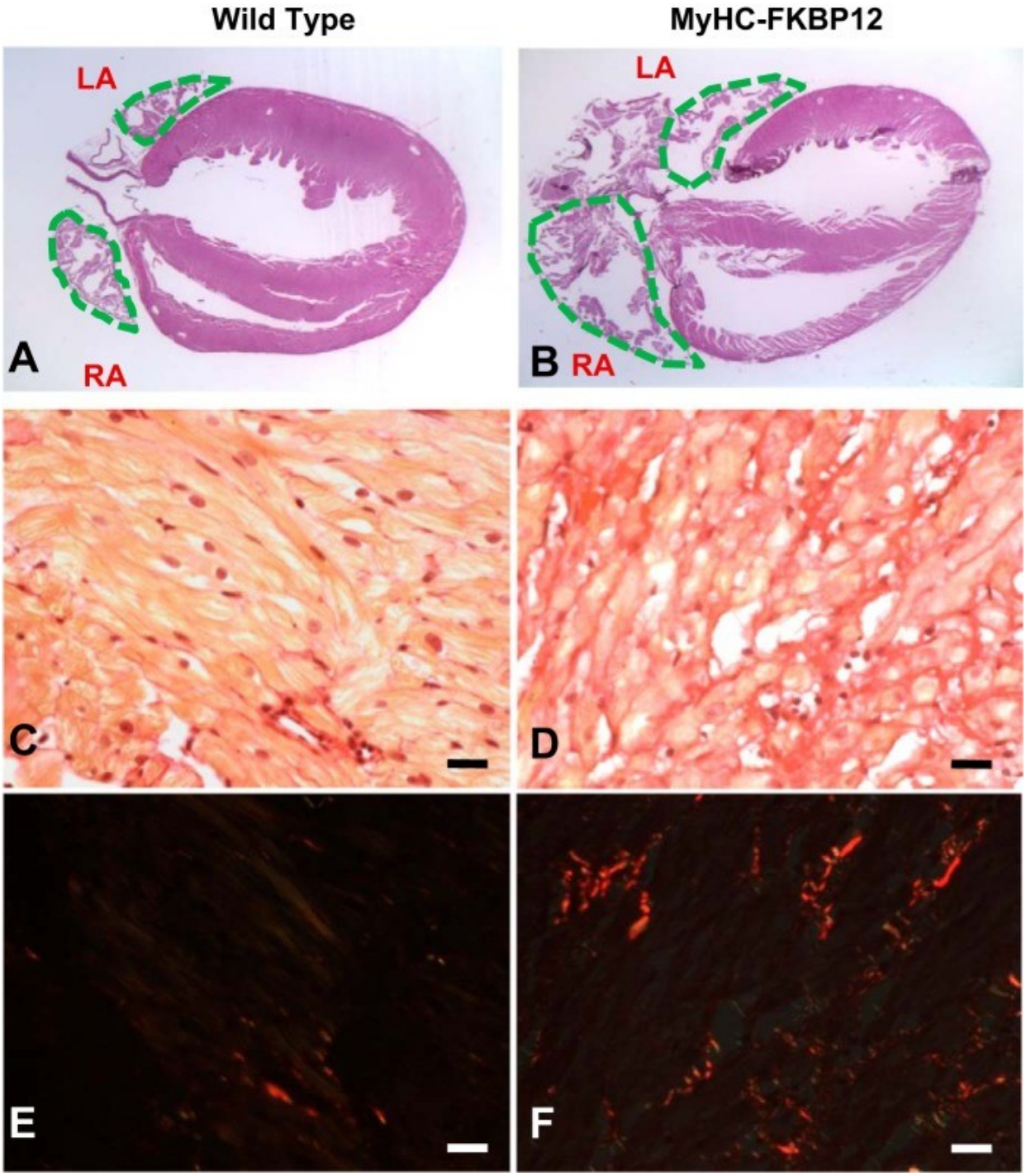

Open in a separate window

A–F: representative histological analysis of the atrial free wall stained with picrosirius red using conventional light (*A–D*) and polarized light (*E* and *F*) from nontransgenic (NTG; *A*, *C*, and *E*) and FK506-binding protein 12 transgenic (αMyHC-FKBP12; *B*, *D*, and *F*) mice. Note the larger atrial size and more abundant interstitial fibrosis in the αMyHC-FKBP12 mouse than in the NTG mouse. Bar = 20 μm. Fibrosis appears red in *E* and *F*. RA, right atria; LA, left atria.